Interlayer and cavity contribution to creating high light-to-solar-gain-ratio glass block from waste glasses

by Prasasto Satwiko

Submission date: 29-Jan-2018 01:33PM (UTC+0700)
Submission ID: 908095601
File name: gh_light-to-solar-gain-ratio_glass_block_from_waste_glasses.pdf (233.46K)
Word count: 5010
Character count: 24699

International Journal of Sustainable Building Technology and Urban Development, 2013
Vol. 4, No. 1, 82–88, http://dx.doi.org/10.1080/2093761X.2012.759891

Interlayer and cavity contribution to creating high light-to-solar-gain-ratio glass block from waste glasses

Floriberta Binarti[a]*, Agustinus Djoko Istiadji[a], Prasasto Satwiko[a] and Priyo Tri Iswanto[b]

[a]*Department of Architecture, University of Atma Jaya Yogyakarta, Jl. Babarsari 44, Yogyakarta 55281, Indonesia;* [b]*Department of Mechanical Engineering, Gadjah Mada University, Jl. Grafika 2, Yogyakarta 55281, Indonesia*

(*Received 30 September 2012; final version received 9 December 2012*)

In order to save building energy consumption, glazing in warm humid climates is recommended to have high light-to-solar-gain ratio (LSG). LSG denotes the ratio of the visible light transmittance (VT) to its solar heat gain coefficient (SHGC). In laminated glazing LSG depends on the design of the cavity and (inter) layers. This study explores the contribution of the interlayers and cavity in creating high LSG glass block from laminated waste glasses. Analytical methods and computational simulations using the comparative method and heat balance model were employed to obtain a glass block model with the optimum combination of VT, SHGC and thermal transmittance (*U*). The cavity effect on the increasing VT is shown by simulation and laboratory test results. Based on SHGC laboratory test results, the presence of an interlayer decreases the simulated SHGC by 69–89%. The LSG for a laminated glass block with a certain number of closed cavities and interlayers can reach 4.35 times the calibrated laboratory LSG.

Keywords: cavity; glass block; interlayer; light-to-solar-gain ratio

1. Introduction

Nowadays many building envelopes are dominated by window glazing. The extensive use of glass produces large volume of waste glasses. Most waste glasses are dumped into landfill sites that burden the environment because they are not biodegradable [1]. Since glass is an ideal material to recycle, reusing or recycling of waste glasses can save significant energy.

The characteristic of ordinary glass, in trapping long-wave solar radiation, makes air-conditioned buildings consume a lot of energy at the operational stage. Adopting high energy performance glazing is a strategy to reduce the solar heat gains. Light-to-solar-gain ratio (LSG) is the prime measure of glazing energy performance in warm humid climates. It represents the ratio of the visible light transmittance (VT) to its solar heat gain coefficient (SHGC). High LSG describes the ability of a glazing to transmit visible light more than the solar radiation. Low thermal transmittance (*U*) glazing is required by air-conditioned buildings. In warm humid climates fenestration with the lowest rise in surface temperature tends to give the best comfort condition [2]. According to Energy Conservation Code 2006 vertical fenestration in warm humid climates should have 0.25 for the maximum SHGC and 3.177 $W/m^2.K$ for the maximum *U* with 0.27 for the minimum VT for small fenestration areas [3].

Lamination was selected as a low-technology method to produce new glass block from waste glasses. It potentially creates low *U* and low SHGC material due to the additional thickness and thermal resistance among the layers. The SHGC, the VT, the *U* and the mechanical strength of the layer bonding depend on the layer number, the interlayer and the lamination technique. This study explores the contribution of the interlayer and cavity to creating high LSG glass block by obtaining and testing the optimum combination of the layer number, and the cavity type, number, width and position. Analytical and computational simulation approaches were employed to obtain new glass blocks with proper cavities. The contribution of the interlayer was observed in laboratory tests.

2. Energy transfer across interlayer and cavity

Limited studies report interlayer contribution to the glazing energy performance. Graphical calculation results of laminated glazing conducted by Powles depict a sharp decline of solar absorption rate and temperature (0.5–0.7 °C) in the Polyvinyl Butyral (PVB) interlayer [4]. However, the low SHGC is created by the presence of low-e coating on the glazing layer surface.

A comparison study on several glazing products [5] shows that increasing the number of glazing layers (with interlayers) can increase the LSG, since the reduction of the SHGC is greater than the VT reduction (Figure 1). Therefore, adding to the number of glazing layers increases the LSG more than adding glazing thickness.

Chen and Meng [6] examined the effect of 7 mm and 11 mm PVB laminated glass application at room base temperature on the building cooling load. Glazing with

*Corresponding author. Email: flo.binarti@gmail.com

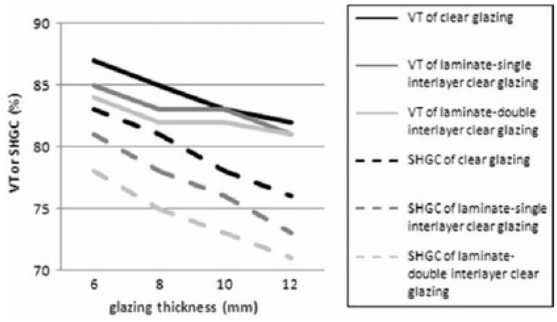

Figure 1. Glazing interlayer effect on the VT and the SHGC.

PVB interlayer has lower SHGC (i.e. 0.510 and 0.430) compared to 12 mm clear glass (i.e. 0.770) and 6 mm low-e coated glass (i.e. 0.610). Although glazing with PVB interlayer tends to have lower VT (i.e. 0.641 and 0.579) compared to clear and low-e glazing (i.e. 0.86 and 0.812), the LSG can be higher, i.e. 1.257 and 1.374. Twelve mm clear glass has 1.12 for the LSG, while the LSG of 6 mm low-e coated glass is 1.33. The simulation results show that PVB laminated glass saves 28% of the building cooling load by preventing 44% of the solar heat gain and reducing the shading coefficient by 40%.

Many studies on glazing cavity were conducted. Evoy and Southall [7] studied the effects of cavity width on the indoor-outdoor temperature differential and the ventilation rate of a supply-air-ventilated window. The effect simulated by computational fluid dynamics (CFD) reaches a very good agreement with experimental data. Simulation and experimental results show that a wider cavity (from 1 cm to 5 cm) reduces the air exit temperature significantly. Meanwhile, a 2 cm-wide cavity achieves the highest convection air flow rate. This effect creates significant reduction of the U value when the cavity width increases from 1 cm to 2 cm. The U value becomes steady for cavity widths greater than 2 cm.

Gosselin and Chen [8] investigated the contribution of cavity in an airflow window to the thermal performance using a CFD program. The window consisted of a triple glazed unit with forced airflow among each glass layer and three varying widths of cavity (9, 12 and 15 mm). Simulation results show that a smaller cavity width creates the best window performance. The influence of cavity width on the vertical temperature difference was also observed in the CFD simulations of an airflow window [9]. An airflow window with a 300 mm cavity width creates an optimum effect on the temperature profile.

The effect of optical and thermal properties of the cavity on the heat transfer rate was examined in a study on conjugate turbulent heat transfer in a square cavity with a solar control coating [10]. It concludes that the total amount of energy transferred to the air in a cavity with a selective coating on the inner side is 41.98% lower than that transferred in a cavity without a selective coating.

A cavity avoids significant reduction of the VT due to its transparency. Material with a higher refractive index (RI) is less transparent [11]. Air has 1 for the RI, whereas clear float glass with a thickness between 2–6 mm has an RI of 1.5189–1.5213. Reduction of the RI depends more on the glazing colour than the thickness [12].

3. Methods

A series of methods was employed to create high LSG glass block from waste glasses. During the process the contribution of the interlayer and cavity can be observed.

3.1 *Cavity type*

The cavity inside glass blocks can be designed as an open cavity or a closed cavity. The CFD-ACE program was used to examine which cavity type creates the lowest indoor temperature. In this study 25 glass blocks with a certain cavity type were arranged as a 1 m^2 vertical fenestration in a 3 m × 3 m × 3 m adiabatic building system. Glass block models were constructed from 285,345 unstructured cell numbers. Unstructured grid generation was selected since it offers maximum flexibility and refines some meshes more easily than structured grid generation. Simulations were conducted with low air velocity (0.1 m/s). The airflow temperature was set to the lowest average temperature (26.85 °C). Heat flux was set to the peak local condition (540 W/m^2), which heated the exterior surface to 50 °C. The low air velocity, the lowest average temperature and the steady state laminar condition were used to describe the significant effect of the convective heat transfer across each model. Convergence was resolved when the residual error reached 0.0001.

Several validation studies support the accuracy of CFD-ACE simulation. Cheng *et al.* [13] investigated the effects of thermal diffusion in laminar jet diffusion flames using CFD-ACE with Reynolds number (Re) = 30 and 330. Comparisons of computed temperature and species concentration profiles of the flames with experimental measurements are in good agreement. Fluid flow and heat transfer of an air-cooled metal foam heat exchanger under a high speed laminar jet confined by two parallel walls were investigated using CFD-ACE with Re = 600–1000 by Ejlali *et al.* [14]. Two numerical solvers had been cross-validated using a Fortran code and CFD-ACE one. The results from the two independent numerical solvers are almost indistinguishable.

3.2 *Analytical approach to estimate U*

Equation (1) was employed to estimate U for each model. This formula was developed from the thermal

transmittance formula and overall thermal resistance formula [2].

$$U = 1/[(1/f_0) + (b_1/k_1) + (b_2/k_2)) + (b_1/k_1) + R+) + (b_1/k_1)) + (b_2/k_2) + (b_1/k_1) + (1/f_i)] \quad (1)$$

The accuracy of the formula depends on the determination of external surface conductance (f_0), internal surface conductance (f_i), thermal resistance of cavity (R), glass conductivity (k_1), interlayer conductivity (k_2), and the layer thickness (b). The first calculation ignored the presence of the interlayer (k_2 and b_2 are 0). Only interlayers among the layers were calculated at the second calculation.

In this study the value of f_0 is 15 W/m^2.K representing external surface conductance in warm humid climates with 3 m/s of air speed, whereas 8.12 W/m^2.K is the internal surface conductance in warm humid climates. The variation in R value depends on the cavity width. The value of k is 1.05 W/m.K for clear glass and 0.1 W/m.K (maximum value) for the interlayer. Clear epoxy resin was chosen as the interlayer material based on its transparency, emissivity, thermal conductivity, compressive and tensile strength, durability, curing time and price. Generally epoxy resin has 0.02–0.1 W/m.K for the thermal conductivity and 0.8 for the emissivity.

3.3 Simulation of the temperature profile

The effects of heat transfer through each model on the airflow rate inside the cavity, and the external and the internal surface temperature were simulated individually by CFD using the same modelling techniques as the previous CFD simulations. Simulations were also conducted to produce temperature profiles of a solid glass block and multilayer glass block with the same thickness and closed cavity design to observe how much the multilayer affects the energy performance. Temperature profiles of 12 multilayer glass block models were also simulated to examine the best energy performance. To lighten the central processing unit (CPU) burden, the interlayer in each model was neglected. This is also valid for other simulations.

3.4 Comparative method of computational simulations

The VT of glass block models was estimated using the comparative method of illumination levels simulated by Radiance (plug in Ecotect). Accuracy of the simulation results relies on the models (the precision degree of the geometry and the reflectivity), ray tracing method [15,16] and simulation setting. Models were constructed to simulate VT field measurement referring to the simulation procedures developed by Laouadi and Arsenault [17]. Each glass block in the VT simulation was installed as a top lighting of a black box with zero reflectance.

The glass block's VT was determined by the ratio of the illumination levels transmitted through each glass block to the illumination level captured by a light sensor in the centre of the black box without glazing. Sky illuminance set up for all simulations is 9897 lux. This condition (normal incidence angle) will create the maximum value of the VT. Validation was conducted using VT field measurement results of single glass and multiple-glasses with and without air gap. The correction factor is 12% higher than simulation results. It was obtained from the deviation value between the simulation results and the field measurement results.

By dividing the simulated direct solar gain of each glass block model ($Q_{g\text{-}glassblock}$) by that of 3 mm standard glass ($Q_{g\text{-}3\,mm}$) the SHGC can be obtained (Equation (2)).

$$SHGC_{glassblock} = (Q_{g-glassblock}/Q_{g-3mm}) \times 0.87 \quad (2)$$

Ecotect (Losses and Gains) was used to calculate the direct solar gain. This facility can analyse heat transfer with the admittance method, which works based on the cyclic variation concept and is valid under steady state conditions. The simulation models were constructed as a horizontal fenestration on a roof plane of a zero U and painted black zone. The simulation date was set on the hottest day.

3.5 Heat balance model

Simulation of heat balance analyses the quantity of the conductive heat gain (Q_c) and Q_g transferred through each glass block model and the internal heat gain produced by a lamp to substitute the lack of daylighting levels (Q_{lamp}). Models were built as a 1 m^2 fenestration on a 3 m × 3 m × 3 m adiabatic room. The internal heat gain was the heat released by the lamp (Q_{lamp}), which was supplemented to reach the same illuminance level as the illuminance level created by 3 mm standard glass application. One watt fluorescent lamp power was assumed to produce an illumination level of 11 lux and 20% of the energy was released as heat. The total heat gain was compared to that of the 3 mm glass. In an adiabatic and air-tight room the indirect solar gain, the interzonal gain, and the ventilation and infiltration gain are zero.

Q_c refers to conductive heat gain (in W) through a surface area in m^2 (A) due to the air temperature differential (in K) between inside (T_i in °C) and outside (T_0 in °C) the space and the thermal transmittance (U) of the surface (Equation (3)).

$$Q_c = U \times (T_0 - T_i) \times A \quad (3)$$

Whereas, Q_g is the direct solar radiation (in W) transmitted through a transparent/translucent surface. It depends on the SHGC of the transparent/translucent surface, the total incident solar radiation on the transparent/translucent surface (E in W/m^2) and the glazing area in m^2 (Equation (4)).

$$Q_g = SHGC \times E \times A \quad (4)$$

3.6 Laboratory tests

VT and SHGC laboratory tests were carried out to measure the real LSG. Measurements of the VT referred to the experimental method developed by Wasley and Utzinger [18] with the average relative error less than 5% compared to the manufacturer's data drawn from the Window 4.1 data base. An artificial lighting (Spotone PAR 80 W) replaced the sun to provide weather-independent measurement, and less shading and reflection effects from the surrounding environment. Luxmeter Lutron LX-101 with 5% accuracy of deviation was used to measure the illuminance level (Figure 2). Laboratory VT was obtained from the ratio of the glass block illuminance level to the illuminance level when no glass was installed on the black-doff box. Validation was conducted by comparing the VT measurement of 5 mm clear glass to the standard VT of 5 mm clear glass.

SHGC measurements were taken using a digital Solar Transmission and Power Meter model SP2065, which has been factory calibrated to a National Institute of Standards and Technology (NIST) traceable thermopile and requires no field adjustment. Self-calibration is carried out by pressing the power mode. Once the display reads P100, the power meter is ready to measure the SHGC of the specimen (Figure 3). The accuracy, therefore, depends on the performance of the control microprocessor and the apparatus position consistency. The comparison of the result of the laboratory SHGC of 5 mm clear glass to the standard value was used to validate the results.

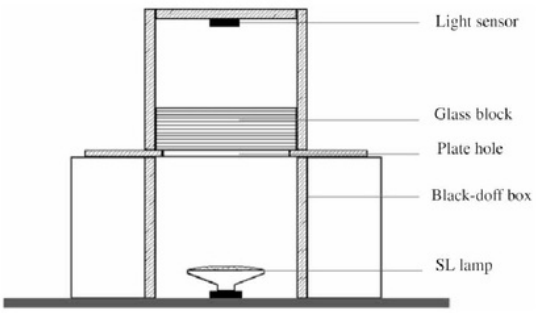

Figure 2. Schematic apparatus of VT laboratory test [19].

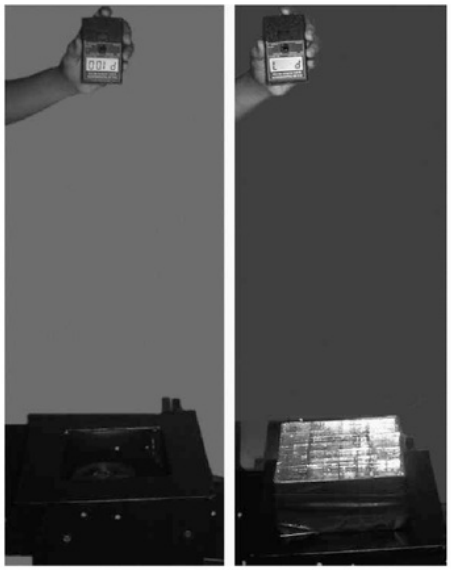

Figure 3. SHGC measurement using Power Meter SP2065: defining the apparatus position (left) and measurement of model l10_l2x2_r1_30 (right) [19].

4. Results and discussions

4.1 Temperature profile created by cavity type

The temperature profile of each model was observed from CFD simulations of glass block models installed as a vertical fenestration of a 9 m^3 building. The model with the closed cavity reaches the lowest indoor temperature (Figure 4). In this case, the closed cavity inside the glass block functions as a thermal insulator. Hot outdoor air flowing inside the open cavity aggravates the high incident solar radiation transmitted through the external glazing layers heating the internal glazing layers. Regarding the results, the glass block with the open cavity is not recommended to be applied in warm humid climates, especially under normal or high thermal conditions.

4.2 Glazing layer and cavity contribution to the energy performance

The simulation result of the multilayer glass block confirms the role of the multilayer in creating low SHGC and U. Figure 5 shows that the multilayer glass block creates a much lower indoor surface temperature (25 °C) compared to the results of the solid glass block (45 °C) with the same thickness and cavity design. The indoor surface temperature difference can reach approximately 20 K.

As a closed cavity creates the best temperature profile, 12 models with various thicknesses, cavity widths, and cavity numbers based on the mechanical strength, the effectiveness of the

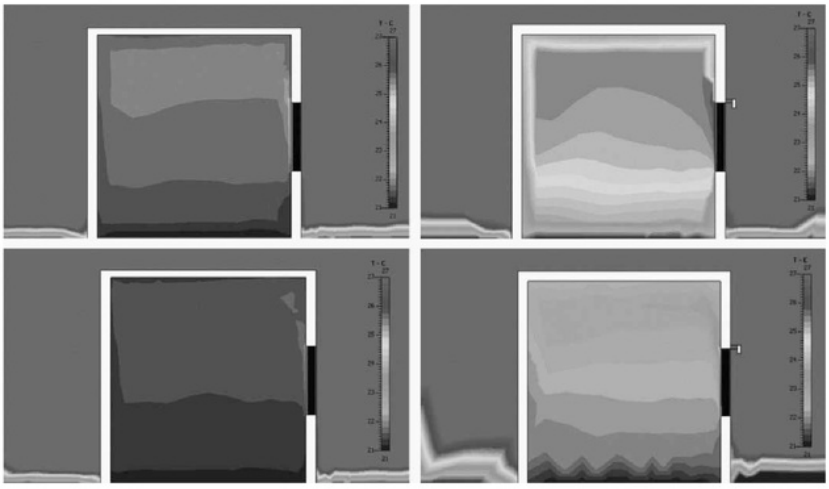

Figure 4. From top left clockwise: Temperature profile of application of glass block without cavity (the average indoor temperature is 21.5 °C), with open cavity (the average indoor temperature is 25 °C), with open cavity in cooler environment (the average indoor temperature is 22.5 °C), and with closed cavity (the average indoor temperature is 21.2 °C) [19].

cavity width and production cost. Table 1 summarises the analytical and computational simulation results of the energy performance of the 12 models. All models have lower U compared to the standard U established by the Conservation Energy Code 2006. The presence of the interlayer decreases U insignificantly. Models with a cavity width of more than 30 mm have relative high SHGC. None of the models exceeded an LSG value of 1. Model l10_l2x2_r1_30 was chosen for further development, since it has the highest LSG, whereas model l18_l3x2_r2_30 was selected due to its combination of the lowest SHGC and a medium VT.

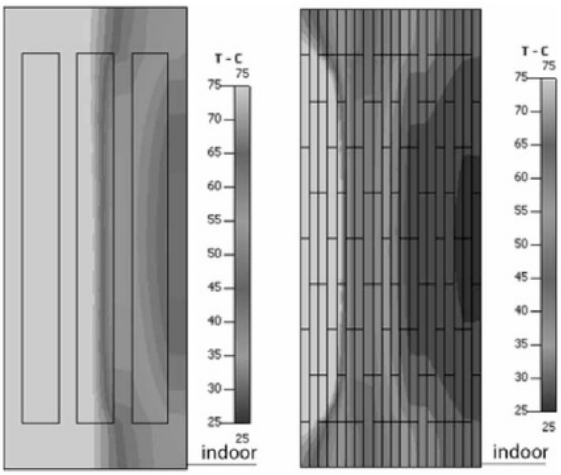

Figure 5. Cross section of a solid glass block (left) and a multilayer glass block (right) with the same thickness and cavity design describing the temperature profile (in °C) simulated by CFD.

Using the heat balance method, application of the best models (i.e. l10_l2x2_r1_30 and l18_l3x2_r2_30 with closed cavity) in the 9 m^3 building model produced much lower heat gain compared to the application of 3 mm clear glass (Table 2). The model with the lowest SHGC (i.e. l18_l3x2_r2_30) produces 16–20% lower Q_g than that of l10_l2x2_r1_30. Two best-model prototypes are presented in Figure 6.

4.3 *Interlayer contribution to the LSG*

The SHGC and VT of each prototype were measured 3–5 times. Table 3 presents laboratory test results of two prototypes with much lower SHGC compared to the simulation results. Low standard deviation of the laboratory SHGC, i.e. 1.2%, proved that the results are valid and reliable. Small reductions occur in the VT with acceptable standard deviation (3.3–4.3%). LSG of real glass blocks increases due to the lower laboratory SHGC than the simulated SHGC. Interlayers in the real glass blocks contribute to decreasing the SHGC more than decreasing the VT.

The big difference between the percentage difference of the simulated SHGC and the laboratory SHGC (Table 4) explains that adding a glazing interlayer reduces the SHGC more than adding a glazing layer. The lower emissivity of the interlayer (0.8) compared to the clear glass emissivity (0.9–0.95) makes the glass block emit less heat to the interior.

Radiance simulation results conform to the VT laboratory test results, which are demonstrated by the small discrepancies between the simulated VT and the VT laboratory test of each model, i.e. 9.6% for model

Table 1. Energy performance of glass block models based on analytical and simulation approach.

Model codes[a]	U_1 (W/m^{2}K)	U_2 (W/m^{2}K)	T_{s_o}[b] (°C)	T_{si}[c] (°C)	VT	SHGC	LSG
l10_l2x2_r1_30	2.60	2.50	77.5	31.5	0.52	0.65	0.80
l11_l2x3_r1_25	2.54	2.44	65.5	30	0.41	0.65	0.63
l12_l2x2_r1_40	3.24	3.14	78	30	0.52	0.74	0.70
l13_l2x3_r1_35	3.17	3.06	67	29	0.40	0.73	0.55
l14_l4x2_r3_10	2.55	2.46	75	28	0.40	0.71	0.56
l14_l3x2_r2_20	2.56	2.20	77.5	28	0.40	0.72	0.56
l15_l3x3_r2_15	2.50	2.17	67	28	0.28	0.70	0.40
l15_l2x3_r1_45	3.06	2.95	67	28	0.40	0.71	0.56
l18_l3x2_r2_30	2.60	2.50	77	27	0.31	0.57	0.54
l19_l3x3_r2_25	2.54	2.44	67	27	0.27	0.59	0.54
l20_l4x2_r3_20	2.30	2.20	78	27	0.31	0.67	0.46
l21_l4x3_r3_15	2.28	2.17	65	27	0.19	0.66	0.29

Note: U_1 = thermal transmittance of a glass block model without interlayer.
U_2 = thermal transmittance of a glass block model with interlayer.
[a] Models are coded using lA_lBxC_rD_E formula, which means that A is the total layer number, B is the glass layer number per group, C is the group number, D is the cavity number, and E is the cavity width in mm.
[b] T_{s0} = outdoor surface temperature
[c] T_{si} = indoor surface temperature

Table 2. Heat balance of best models.

Models	Q_c (W)	Q_g (W)	$Q_c + Q_g$ (W)	Q_{lamp} (W)	Q_{total} (W)	Efficiency (%)
			Oriented to West			
l10_l2x2_r1_30	142.0	213.7	355.7	5.8	361.5	60
l18_l3x2_r2_30	142.0	98.0	239.9	6.2	246.1	70
3 mm clear glass	322.2	655.4	977.5	0.0	977.5	0
			Oriented to South			
l10_l2x2_r1_30	142.0	106.5	248.4	5.8	254.3	60
l18_l3x2_r2_30	142.0	48.8	190.8	6.2	197.0	70
3 mm clear glass	322.2	326.5	648.7	0.0	648.7	0
			Oriented to East			
l10_l2x2_r1_30	142.0	328.4	470.3	5.8	476.2	60
l18_l3x2_r2_30	142.0	150.5	292.5	6.2	298.7	80
3 mm clear glass	322.2	1006.8	1328.9	0.0	1328.9	0
			Oriented to North			
l10_l2x2_r1_30	142.0	206.3	348.2	5.8	354.1	60
l18_l3x2_r2_30	142.0	94.5	236.5	6.2	242.7	70
3 mm clear glass	322.2	954.6	954.6	0.0	954.6	0

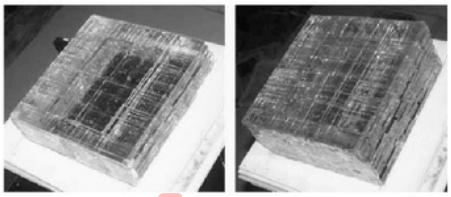

Figure 6. Prototype of model l10_l2x2_r1_30 (left) and model l18_l3x2_r2_30 (right) [19].

l10_l2x2_r1_30 and 3.2% for l18_l3x2_r2_30. These discrepancies appear due to the imprecision of the model geometry more than the accuracy of Radiance in calculating interreflections among glazing layers. Therefore, the presence of interlayers in real glass blocks affects the VT insignificantly. The less transparent (higher RI) interlayer compared to the clear glass creates a small (percentage) difference between the simulated VT and the laboratory VT.

Table 3. Laboratory test results of the VT and the SHGC.

Properties	l10_l2x2_r1_30	l18_l3x2_r2_30
Calibrated lab. VT	0.47	0.30
Standard deviation of lab. VT	4.30%	3.30%
Simulated VT	0.52	0.31
Calibrated SHGC	0.18	0.06
Standard deviation of laboratory SHGC	1.20%	1.20%
Simulated SHGC	0.65	0.57
Laboratory LSG	2.50	4.35

Table 4. Percentage difference between two glass blocks.

Properties	l10_l2x2_r1_30	l18_l3x2_r2_30	Percentage Difference
Simulated SHGC	0.65	0.57	12%
Laboratory SHGC	0.18	0.06	67%
Simulated VT	0.52	0.31	40%
Laboratory VT	0.47	0.30	36%
Simulated LSG	0.80	0.54	32%
Laboratory LSG	2.50	4.35	(-) 74%

5. Conclusions

A closed cavity with medium width (25–30 mm) in a laminated glass block admits optimum visible light and low solar radiation. The cavity width should be no more than 30 mm to avoid high SHGC. SHGC and indoor surface temperature also depend on the glass block's thickness. Collaboration between interlayer and multilayer reduces material consumption in creating new material with low SHGC and *U*. The presence of an interlayer (epoxy resin) in a laminated glass block reduces the SHGC significantly with a small reduction in the VT. Interlayer contribution to decreasing of the SHGC depends on the emissivity. Certain combinations of closed cavity and interlayer number help the glass block reach high LSG. New interlayers with lower emissivity and lower refractive index will create a higher energy performance laminated glass block.

Acknowledgements

This research was supported by the Directorate General of Higher Education (Dirjen DIKTI), Ministry of National Education in the scheme of "National Research Competitive Grant" (Hibah Bersaing) under the contract no. 055/SP2H/PP/DP2M/IV/2009 on April 6, 2009 and no. 301/SP2H/P/DP2M/IV/2010 on April 12, 2010. Authors are also grateful to Mr. Widijanto (laboratory staff) for preparing the specimens.

References

[1] P. Turgut and E.S. Yahlizade, *Research into concrete blocks with waste glass*, Environ. Sci. Eng. 1 (2009), pp. 202–208.
[2] ASHRAE *ASHRAE Handbook: Fundamental, Inch-Pound Edition*, ASHRAE, Atlanta, GA, 2009.
[3] International Institute for Energy Conservation (IIEC) and United States Agency for International Development (USAID) *Energy Conservation Building Code 2006*, Bureau of Energy Efficiency, New Delhi, 2006.
[4] R. Powles, D. Curcija, and C. Kohler, *Solar absorption in thick and multilayer glazings*, Proc. the World Renewable Energy Congress VII, Cologne, 2002.
[5] N.C. Stokes, *G. James is Glass Handbook*, 1st ed. 1998, Available at http://gjames.com/__data/assets/pdf_file/0005/49307/gjames_glass_handbook.pdf
[6] Z. Chen and Q. Meng, *Analysis and research on the thermal properties of energy-efficient building glass: A case study on PVB laminated glass*, Proc. Sixth International Conference for Enhanced Building Operations, Shenzhen, ESL-IC-06-11-58, 2006.
[7] M. Evoy and R.G. Southall, *Validation of a Computational Fluid Dynamics Simulation of a Supply Air Ventilated Window*, Proc. 20/20 Vision CIBSE/ASHRAE conference, Dublin, 2000. Available at http://www.cibse.org/pdfs/Validation%20of%20CFD%20sim.pdf
[8] J.R. Gosselin and Q. Chen, *A dual airflow window for indoor air quality improvement and energy conservation in buildings*, Int. J. HVAC & R Res. 14 (2008), pp. 359–372.
[9] M. Ghadimi, H. Ghadamian, A.A. Hamid, F. Fazelpour, and M.A. Behghadam, *Analysis of free and forced convection in airflow window using numerical simulation of heat transfer*, Int. J. Energy Environ. Eng. (2012), 3(14), doi: 10.1186/2251-6832-3-14. Available at http://www.journal-ijeee.com/content/3/1/14
[10] J. Xaman, G. Alvarez, J. Hinojosa, and J. Flores, *Conjugate turbulent heat transfer in a square cavity with a solar control coating deposited to a vertical semitransparent wall*, Heat Fluid Flow 30 (2009), pp. 237–248.
[11] E. Hecht, *Optics*, Addison-Wesley, Boston, 2002.
[12] U.K. Ahmad, N.F. Asmuje, R. Ibrahim, and N.U. Kamaruzaman, *Forensic classification of glass employing refractive index measurement*, Malays. J. Forensic Sci. 3 (2012), pp. 1–4.
[13] T.S. Cheng, C.-Y. Wu, C.-P. Chen, Y.-H. Li, Y.-C. Chao, T. Yuan, and T.S. Leu, *Detailed measurement and assessment of laminar hydrogen jet diffusion flames*, Combust. Flame 146 (2006), pp. 268–282.
[14] Az. Ejlali, Ar. Ejlali, K. Hooman, and H. Gurgenci, *Application of high porosity metal foams as air cooled heat exchangers to high heat load removal system*, Int. Commun. Heat Mass Transfer 36 (2009), pp. 674–679.
[15] J. Mardaljevic, *Verification of program accuracy for illuminance modeling: Assumptions, methodology and an examination of conflicting findings*, Light. Res. Technol. 36 (2004), pp. 218–238.
[16] C.F. Reinhart and M. Andersen, *Development and validation of a Radiance model for a translucent panel*, Energy Build. 38 (2006), pp. 890–904.
[17] A. Laouadi and C. Arsenault, *Validation of skylight performance assessment software*, ASHRAE Transactions 112 (2006), pp. 1–13.
[18] J.H. Wasley and M. Utzinger, *Vital Signs 2*, (1996), Available at http://arch.ced.berkeley.edu/vitalsigns/res/downloads/rp/glazing/glaz1-bg.pdf
[19] Binarti, F., Istiadji, A.D., Satwiko, P., & Iswanto, P.T. Raising high energy performance glass block from waste glasses with cavity and interlayer. 4th International Conference on Sustainability in Energy and Buildings, Stockholm, 2012.

Interlayer and cavity contribution to creating high light-to-solar-gain-ratio glass block from waste glasses

GRADEMARK REPORT

FINAL GRADE

/40

GENERAL COMMENTS

Instructor

PAGE 1

PAGE 2

PAGE 3

PAGE 4

PAGE 5

PAGE 6

PAGE 7

Interlayer and cavity contribution to creating high light-to-solar-gain-ratio glass block from waste glasses

ORIGINALITY REPORT

19%	16%	12%	7%
SIMILARITY INDEX	INTERNET SOURCES	PUBLICATIONS	STUDENT PAPERS

PRIMARY SOURCES

1	es.scribd.com Internet Source	3%
2	seb12.sustainedenergy.org Internet Source	2%
3	I. V. Miroshnichenko, M. A. Sheremet. "Turbulent Natural Convection and Surface Radiation in a Closed Air Cavity with a Local Energy Source", Journal of Engineering Physics and Thermophysics, 2017 Publication	1%
4	Cai, Jian, Shenghui Lei, Adhiraj Dasgupta, Michael F. Modest, and Daniel C. Haworth. "High fidelity radiative heat transfer models for high-pressure laminar hydrogen–air diffusion flames", Combustion Theory and Modelling, 2014. Publication	1%
5	Esmailie, F., H. Ghadamian, and M. Aminy. "Modeling and simulation of a solar flat plate	1%

collector as an air heater considering energy efficiency", Mechanics & Industry, 2014.
Publication

6	www.tandfonline.com Internet Source	1%
7	Hu, Haitao, Zhancheng Lai, Xiaomin Weng, Guoliang Ding, and Dawei Zhuang. "Numerical model of dehumidifying process of wet air flow in open-cell metal foam", Applied Thermal Engineering, 2017. Publication	1%
8	Bo Sun, , Jianing Zhao, and Jingshu Wei. "Analysis of indoor occupant contaminants under the isothermal dual-airflow window ventilation", 2011 International Conference on Electric Technology and Civil Engineering (ICETCE), 2011. Publication	1%
9	oaktrust.library.tamu.edu Internet Source	1%
10	www.scipedia.com Internet Source	<1%
11	inis.iaea.org Internet Source	<1%
12	docs.lib.purdue.edu Internet Source	<1%

13	arts.brighton.ac.uk Internet Source	<1%
14	Jones, Nathaniel L., and Christoph F. Reinhart. "Experimental validation of ray tracing as a means of image-based visual discomfort prediction", Building and Environment, 2016. Publication	<1%
15	Submitted to Universiti Teknologi Malaysia Student Paper	<1%
16	journal.ui.ac.id Internet Source	<1%
17	Submitted to University of Nottingham Student Paper	<1%
18	arch.ced.berkeley.edu Internet Source	<1%
19	studentsrepo.um.edu.my Internet Source	<1%
20	e-journal.uajy.ac.id Internet Source	<1%
21	Ille, Mario, Jure Radić, and Jelena Bleiziffer. "Design and assessment of concrete surface protection systems", International Journal of Sustainable Building Technology and Urban Development, 2013. Publication	<1%

22	Ling, T.C.. "Feasibility of using recycled glass in architectural cement mortars", Cement and Concrete Composites, 201109 Publication	<1%
23	Ejlali, A.. "Application of high porosity metal foams as air-cooled heat exchangers to high heat load removal systems", International Communications in Heat and Mass Transfer, 200908 Publication	<1%
24	www.ripublication.com Internet Source	<1%
25	Submitted to Cranfield University Student Paper	<1%
26	eprints.ners.unair.ac.id Internet Source	<1%
27	www.chemweb.com Internet Source	<1%
28	documents.mx Internet Source	<1%
29	Jennifer Gosselin. "A Dual Airflow Window for Indoor Air Quality Improvement and Energy Conservation in Buildings", HVAC&R Research, 05/01/2008 Publication	<1%

30	Submitted to University of Northampton Student Paper	<1%
31	Kumar, Devander, and Sudhir Kumar. "Year-round performance assessment of a solar parabolic trough collector under climatic condition of Bhiwani, India: A case study", Energy Conversion and Management, 2015. Publication	<1%
32	www.thefreelibrary.com Internet Source	<1%
33	www.samsi.no Internet Source	<1%
34	Beñat Arregi, Roberto Garay. "Regression analysis of the energy consumption of tertiary buildings", Energy Procedia, 2017 Publication	<1%
35	Acosta, I.. "Daylighting design with lightscoop skylights: Towards an optimization of proportion and spacing under overcast sky conditions", Energy & Buildings, 201206 Publication	<1%
36	Floriberta Binarti, Sinta Dewi. "The Effectiveness of Light Shelf in Tropical Urban Context", Environmental and Climate Technologies, 2016 Publication	<1%

37	Submitted to University of Bath Student Paper	<1%
38	Cheng, T.S.. "Further analysis of chemical kinetic structure of a standoff microjet methane diffusion flame near extinction", Combustion and Flame, 200802 Publication	<1%
39	Cheng, T.S.. "Detailed measurement and assessment of laminar hydrogen jet diffusion flames", Combustion and Flame, 200607 Publication	<1%

Exclude quotes	Off	Exclude matches	Off
Exclude bibliography	Off		